Eur. Phys. J. A (2013) **49**: 92
DOI 10.1140/epja/i2013-13092-9

THE EUROPEAN PHYSICAL JOURNAL A

Regular Article – Experimental Physics

Lifetime measurements of ^{214}Po and ^{212}Po with the CTF liquid scintillator detector at LNGS

Borexino Collaboration

G. Bellini[1], J. Benziger[2], D. Bick[3], G. Bonfini[4], D. Bravo[5], M. Buizza Avanzini[1], B. Caccianiga[1], L. Cadonati[6], F. Calaprice[7], C. Carraro[8], P. Cavalcante[4], A. Chavarria[7], A. Chepurnov[9], V. Chubakov[10], D. D'Angelo[1], S. Davini[8], A. Derbin[11], A. Etenko[12], K. Fomenko[4,13], D. Franco[14], C. Galbiati[7], S. Gazzana[4], C. Ghiano[4], M. Giammarchi[1], M. Göger-Neff[15], A. Goretti[7], L. Grandi[7], E. Guardincerri[8], S. Hardy[5], Aldo Ianni[4], Andrea Ianni[7], V. Kobychev[16], D. Korablev[13], G. Korga[4], Y. Koshio[4], D. Kryn[14], M. Laubenstein[4], T. Lewke[15], Marcello Lissia[17,a], E. Litvinovich[12], B. Loer[7], F. Lombardi[4], P. Lombardi[1], L. Ludhova[1], I. Machulin[12], S. Manecki[5], W. Maneschg[18], G. Manuzio[8], Q. Meindl[15], E. Meroni[1], L. Miramonti[1], M. Misiaszek[19], D. Montanari[20], P. Mosteiro[7], F. Mantovani[10], V. Muratova[11], S. Nisi[4], L. Oberauer[15], M. Obolensky[14], F. Ortica[21], K. Otis[6], M. Pallavicini[8], L. Papp[4,5], L. Perasso[1], S. Perasso[8], A. Pocar[6], G. Ranucci[1], A. Razeto[4], A. Re[1], A. Romani[21], N. Rossi[4], A. Sabelnikov[12], R. Saldanha[7], C. Salvo[8], S. Schönert[15,18], H. Simgen[18], M. Skorokhvatov[12], O. Smirnov[13], A. Sotnikov[13], S. Sukhotin[12], Y. Suvorov[4,12], R. Tartaglia[4], G. Testera[8], R.B. Vogelaar[5], F. von Feilitzsch[15], J. Winter[15], M. Wojcik[19], A. Wright[7], M. Wurm[15], G. Xhixha[10], J. Xu[7], O. Zaimidoroga[13], S. Zavatarelli[8], and G. Zuzel[18,19]

[1] Dipartimento di Fisica, Università and INFN, Milano 20133, Italy
[2] Chemical Engineering Department, Princeton University, Princeton, NJ 08544, USA
[3] Institut für Experimentalphysik, Universität Hamburg, Germany
[4] INFN Laboratori Nazionali del Gran Sasso, Assergi 67010, Italy
[5] Physics Department, Virginia Polytechnic Institute and State University, Blacksburg, VA 24061, USA
[6] Physics Department, University of Massachusetts, Amherst MA 01003, USA
[7] Physics Department, Princeton University, Princeton, NJ 08544, USA
[8] Dipartimento di Fisica, Università and INFN, Genova 16146, Italy
[9] Institute of Nuclear Physics, Lomonosov Moscow State University, 119899, Moscow, Russia
[10] Dipartimento di Fisica, Università and INFN, I-44100 Ferrara, Italy
[11] St. Petersburg Nuclear Physics Institute, Gatchina 188350, Russia
[12] NRC Kurchatov Institute, Moscow 123182, Russia
[13] Joint Institute for Nuclear Research, Dubna 141980, Russia
[14] APC, Univ. Paris Diderot, CNRS/IN2P3, CEA/Irfu, Obs de Paris, Sorbonne Paris Cité, France
[15] Physik Department, Technische Universität München, Garching 85747, Germany
[16] Kiev Institute for Nuclear Research, Kiev 06380, Ukraine
[17] INFN, Sezione di Cagliari, I-09042 Monserrato, Italy
[18] Max-Plank-Institut für Kernphysik, Heidelberg 69029, Germany
[19] M. Smoluchowski Institute of Physics, Jagiellonian University, Krakow, 30059, Poland
[20] Fermi National Accelerator Laboratory, Batavia, IL 60510, USA
[21] Dipartimento di Chimica, Università and INFN, Perugia 06123, Italy

Received: 11 January 2013 / Revised: 23 May 2013
Published online: 18 July 2013

Communicated by E. Bellotti

Abstract. We have studied the α-decays of ^{214}Po into ^{210}Pb and of ^{212}Po into ^{208}Pb tagged by the coincidence with the preceding β-decays from ^{214}Bi and ^{212}Bi, respectively. The ^{222}Rn, ^{232}Th, and ^{220}Rn sources used were sealed inside quartz vials and inserted in the Counting Test Facility at the underground Gran Sasso National Laboratory in Italy. We find that the mean lifetime of ^{214}Po is $(236.00 \pm 0.42(\text{stat}) \pm 0.15(\text{syst}))\,\mu$s and that of ^{212}Po is $(425.1 \pm 0.9(\text{stat}) \pm 1.2(\text{syst}))$ ns. Our results, obtained from data with signal-to-background ratio larger than 1000, reduce the overall uncertainties and are compatible with previous measurements.

[a] e-mail: marcello.lissia@ca.infn.it

Table 1. Existing measurements of the ^{214}Po half-life and compilations compared to the present work.

Reference	Half-life (μs)
von Dardel (1950) [2]	163.7 ± 0.2
Ballini (1953) [3]	158.0 ± 2.0
Ogilvie (1960) [4]	159.5 ± 3.0
Dobrowolski (1961) [5]	164.3 ± 1.8
Erlik (1971) [6]	165.5 ± 3.0
Zhou (1993) [7]	160.0 ± 12.0
Alexeyev (2013) [8]	163.5 ± 0.8[a]
Nuclear Data Sheet (2009) [9]	164.3 ± 2.0[b]
Table de Radionucléides (2007) [10]	162.3 ± 1.2[c]
This work (2012)	$\mathbf{163.6 \pm 0.3}$

[a] Average of the two values, 162.73 and 164.25, reported in ref. [8]; since systematic errors of these measurements are still under study [8] the uncertainty is estimated as (164.25–162.73)/2.
[b] Average of [2], [5] and [6] with the original uncertainty of [2] increased to 2 μs; used in the *Table of Isotopes*.
[c] Average of all six values, with the original uncertainty of [2] increased to 1.8 μs.

Table 2. Existing measurements of the ^{212}Po half-life and compilations compared to the present work.

Reference	Half-life (ns)
Bunyan (1949) [11]	304 ± 4
Flack (1962) [12]	305 ± 25
Astner (1963) [13]	305 ± 5
McBeth (1972) [14]	304 ± 8[a]
McBeth (1972) [14]	300 ± 8[b]
Sanyal (1975) [15]	296 ± 2
Bohn (1981) [16]	309 ± 11
Table of Isotopes (2005) [17]	299 ± 2[c]
Table de Radionucléides (2010) [18]	300 ± 2[d]
This work (2012) first source	$\mathbf{295.6 \pm 1.3}$
This work (2012) second source	$\mathbf{294.0 \pm 1.1}$
This work (2012) combined	$\mathbf{294.7 \pm 1.0}$

[a] Curve (A) of fig. 4 in ref. [14].
[b] Curve (B) of fig. 4 in ref. [14].
[c] Average of [11], [13], [14] (curve (A) of fig. 4), [15], and [16].
[d] Average of [11], [12], [13], [14] (both curves (A) and (B) of fig. 4), [15], and [16], with the original uncertainty of [15] increased to 2.7 ns.

1 Introduction

Both ^{214}Po and ^{212}Po are polonium unstable isotopes, characterized by short mean-lives ($\tau_{^{214}\mathrm{Po}} \approx 235\,\mu$s, $\tau_{^{212}\mathrm{Po}} \approx 430$ ns) and by emission of alpha particles with energies $E_{^{214}\mathrm{Po}} \approx 7.833$ MeV and $E_{^{212}\mathrm{Po}} \approx 8.954$ MeV and practically 100% branching ratios (BR). They belong to the ^{238}U and ^{232}Th chains, respectively. In this work, we report on the precise measurements of the ^{214}Po and ^{212}Po mean-lives, performed with the Counting Test Facility (CTF) [1], a ≈ 1 ton liquid scintillator detector installed at the underground Gran Sasso National Laboratory (LNGS) in Italy. In both measurements, we look for the fast coincidence between the β-decay of the father isotope (^{214}Bi or ^{212}Bi) and the ^{214}Po or ^{212}Po α-decay, respectively. The ^{214}Po lifetime measurement is characterized by unprecedented large statistics ($\approx 10^5$ events), and both the ^{212}Po and ^{214}Po measurements exploit a very long acquisition window (≈ 7 mean-lives). Moreover, the high purity of the detector materials makes it possible to reach a signal-to-background ratio three orders of magnitude better than the other existing measurements listed in tables 1 and 2.

2 The experimental setup

2.1 The measurement principle

The α particles from ^{212}Po and ^{214}Po decays are tagged via the coincidence with β's from ^{212}Bi and ^{214}Bi. The ^{212}Bi is characterized by a β-decay with $\approx 64\%$ BR and Q-value of ≈ 2.254 MeV, while ^{214}Bi β-decay has almost 100% BR and 3.272 MeV Q-value. The times elapsed between the prompt β and delayed α events are driven by the decay times of polonium and are therefore short (a few hundreds microseconds for ^{214}Po and a few hundreds nanoseconds for ^{212}Po). The CTF electronics are able to detect such time differences with high precision. The space-time coincidence condition provides a very clean event signature. In comparison with other measurements of this kind, the background level is further suppressed by the high radio-purity of the CTF detector [19].

2.2 The Counting Test Facility

A detailed description of CTF can be found in [1], while here we only recall those detector features that are important for the particular measurement presented in this paper. The external cylindrical tank (≈ 11 m diameter, ≈ 10 m height) was filled with about 1000 tons of water serving as a passive shield against external neutrons and γ's. The core of the detector was represented by 4.8 m^3 of liquid organic scintillator (LS)[1] contained in a spherical inner vessel (IV) of ≈ 2 m diameter. The IV was realized in $\approx 500\,\mu$m thick nylon membrane with excellent optical clarity, which allowed the effective transmission of the scintillation light to the 100 photomultiplier tubes (PMTs) performing the optical read-out. These 8 inch ETL 9351 PMTs, which were anchored on a 7 m diameter support

[1] Binary mixture of the aromatic liquid 1-2-4 trimethyl benzene (pseudocumene or PC) as solvent and the fluor admixture of 2,5-diphenyloxasol (PPO) with about 1.5 g/l concentration.

structure placed inside the water tank, had $\approx 26\%$ quantum efficiency at 420 nm, a limited transit time spread ($\sigma \approx 1$ ns), and a good pulse height resolution for single photoelectron pulses (Peak/Valley ≥ 2.5). Light concentrators (57 cm long and 50 cm diameter aperture) mounted on the PMTs enhanced the optical coverage to about 20%.

The fluorescence maximum is at 365 nm. The yield of emitted photons was $\approx 10^4$ per MeV of deposited energy, while the measured light yield corresponded on average to 380 photoelectrons (p.e.) collected by 100 PMT's per 1 MeV of energy deposit. For each trigger (event), the charge and timing (1 ns precision) of all hit PMTs were recorded. Each electronics channel was paired with an auxiliary channel of equal characteristics, able to record a possible second event occurring within an 8 ms time window. The parameters reconstructed for each event were: the total charge collected by the PMTs during a 500 ns time interval in order to infer the energy deposit, the time distribution of hit PMTs used for the pulse shape discrimination and for the event position reconstruction (resolution of 10–15 cm), and the time elapsed between sequential events, used for the precise time difference measurement between correlated events.

A special insertion system installed on the top of the CTF made it possible to place suitable radioactive sources inside the detector without contaminating the LS. The pipe of the insertion system had an internal diameter of 50 mm. The positioning of the sources was done by means of steerable aluminum rods. The ^{214}Po and ^{212}Po sources were placed at the detector center and its exact positions were later determined via the position reconstruction code which had a precision of a few centimeters.

2.3 Preparation of the sources

The ^{214}Po and ^{212}Po sources were prepared by dissolving the suitable isotopes in the LS, which was contained in the vials with an external diameter of 50 mm, the maximum allowed by the insertion system. The vials were made of quartz, which is transparent to UV light. The LS used in the source preparation was drawn directly from the CTF inner vessel in order to ensure the same optical properties in terms of the light yield and quenching effects. In order to minimize a possible contamination with oxygen, which acts as a quencher with a consequent light-yield reduction, the LS withdrawal was performed under a controlled high-purity nitrogen atmosphere [20]. These sources have been prepared with the purpose of studying anti-neutrino spectra important in geoneutrino studies as discussed in [21].

2.3.1 Preparation of the ^{214}Po source

The vial employed for the ^{214}Po source was a 50 mm diameter sphere with ≈ 1 mm wall thickness. The source was realized by spiking the LS with ^{222}Rn obtained from a ^{226}Ra-based "radon generato" and having the ^{214}Bi-^{214}Po sequence within its decay chain. The ^{222}Rn half-life of 3.824 days is long enough to allow the realization of an effective spiking procedure. To maintain the mandatory oxygen-free conditions of the scintillator, we built a dedicated system allowing the Rn influx into the vial under a strictly controlled flow of high-purity nitrogen. The Rn solubility in the PC is high enough to allow an efficient capture of the radioisotope into the scintillator.

The required total source activity was about 10 Bq. Such a low counting rate matches the electronics maximum read-out (the electronics dead-time is 110–120 ms, slightly dependent on energy) and also excludes the possibility of saturation and/or pile-up effects. Such a low-activity source was obtained by dissolving a few ml of 8000 Bq mother solution (Radon dissolved in PC) in the LS. The mother solution can have higher oxygen contamination than the original LS. The concept of high-activity mother solution makes it possible to minimize the amount used in the source preparation. The data taking started immediately after inserting the 10 Bq source in the CTF and it was stopped when the source activity decayed to a few Bq.

2.3.2 Preparation of the two ^{212}Po sources

The mere replication of the procedure adopted for ^{214}Po was not possible, since ^{220}Rn, the radon progenitor of the ^{212}Bi, has a half-life of only 55.6 s. Two alternative methods, described below, were used instead in order to prepare two different ^{212}Po sources.

A) *First* ^{212}Po *source*

In this approach we used the fact that ^{212}Po is a member of the ^{232}Th decay chain. We employed natural thorium dissolved in nitric acid at 2%. Since thorium is insoluble in PC, we had to use TriButyl Phosphate (TBP) to form stable hydrophilic complexes of thorium. These compounds are soluble in organic solvents and were mixed in the scintillator that was inserted into the vial. The concentration of thorium in TBP was measured by inductively coupled plasma mass spectrometry to be about 100 ppb corresponding roughly to 43 Bq/kg. The TBP concentration was kept below 5% according to fluorimetric measurements to minimize quenching effects. In order to accumulate sufficient statistics, we increased the source volume; we built a cylindrical quartz vial 20 cm high and with the maximum diameter allowed by the insertion system for a total volume of about 300 cm^3.

The ^{212}Po source had a total activity of about half a Bq; it did not change significantly during the data taking, which lasted a short time compared to the ^{232}Th half-life of about 14 billion years.

B) *Second* ^{212}Po *source*

As an alternative method avoiding the TBP dilution into the scintillator, a second source was prepared using a system able to transfer ^{220}Rn gas directly into the spherical quartz vial. We again used natural thorium dissolved in nitric acid at 2%. The core of the system was an extraction chamber, a 40 cm high stainless-steel cylinder with 16 mm

internal diameter, containing 20 cm^3 of aqueous solution with $\approx$ 1 g/l of dissolved natural thorium with 80 Bq of total activity. High-purity nitrogen was fluxed into the extraction chamber, in order to bubble the aqueous solution and to transfer the emanated ^{220}Rn to the scintillator contained in the vial. The high-purity nitrogen loaded with ^{220}Rn was flushed inside a 7 m long nylon tube with 2 mm internal diameter. Because of its short lifetime, only a fraction of the original ^{220}Rn reached the vial. A nylon trap was inserted on top of the extraction chamber to avoid potential water contamination of the scintillator. The 2 mm nylon tube was contained inside a second nylon tube of 6 mm internal diameter, that acted both as nitrogen exhaust and as a tether for the quartz vial. Since both tubes were flexible, a 3 kg stainless-steel cylindrical weight was positioned just above the vial in order to hold its position in the CTF center. The nitrogen flux was set to 10 liters per hour with a corresponding gas velocity inside the 2 mm nylon of about 90 cm/s. The expected ^{212}Bi activity in the vial was about 4 Bq. Given that the half-life of ^{212}Pb is about 10.6 h, the desired ^{212}Po activity was built up after approximately 20–30 hours.

3 Data analysis and results

The total live-time of data taking for the ^{214}Po measurement is 10.2 d. For the two ^{212}Po sources, the live-times are 6.3 d and 15.5 d, respectively. The correspondent overall statistics are $\approx 3.9\times10^5$ ^{214}Po and $\approx (1.1+1.7)\times10^5$ ^{212}Po candidates for the first and second source, respectively. The two ^{212}Po candidate samples from the two sources are analyzed independently.

The energy response of the detector is calibrated run by run, using the light yield obtained by fitting the ^{14}C energy spectrum: on average 3.8 p.e. per PMT are detected for a 1 MeV recoiling electron at a random position within the detector volume [22]. In these measurements, the yields are 240 p.e./MeV and 220 p.e./MeV with 70 PMTs for the ^{214}Po and ^{212}Po analyses, respectively. The reduced yields are due to impurities, such as oxygen in the ^{214}Po vial and thorium salts in the ^{212}Po vial, which act as light quenchers. The ^{214}Bi-^{214}Po and ^{212}Bi-^{212}Po (source 1 and 2) energy spectra are shown in figs. 1, 2, and 3. These figures also show that the measured light yield from alpha particles (polonium decays) are quenched by a factor $\approx$ 10–15 with respect to electron equivalents.

A time threshold of 400 ns for the ^{212}Bi $\rightarrow$ ^{212}Po decay sample was imposed to avoid the scintillation tail of the first event. A threshold of 5 μs was applied for the ^{214}Bi $\rightarrow$ ^{214}Po decay sample in order to avoid background from ^{212}Bi $\rightarrow$ ^{212}Po decays with a lifetime of about 0.4 μs, naturally present in the scintillator.

The data analysis relies on a triple approach in order to cross check the results and to minimize the errors. Results from these approaches are summarized in table 3 and described below.

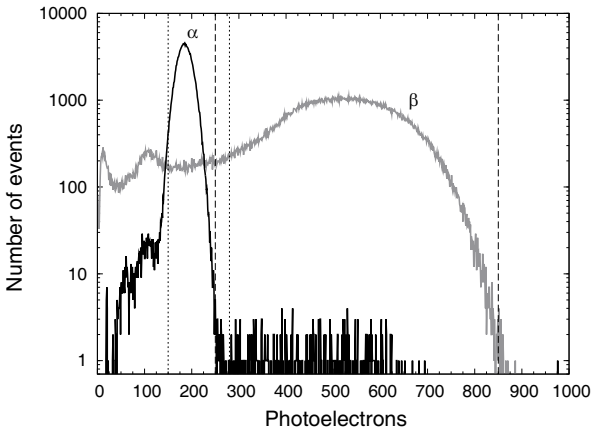

Fig. 1. Energy spectrum for the prompt (candidate β-decay of ^{214}Bi, gray histogram) and delayed event (candidate α-decay of ^{214}Po, black histogram) of TCE. Vertical dashed (dotted) lines delimit energy cuts for the β (α) candidates used in the analysis.

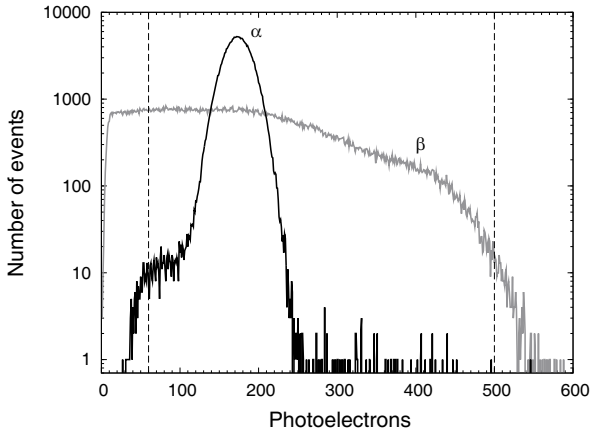

Fig. 2. Energy spectrum for the prompt (candidate β-decay of ^{212}Bi, gray histogram) and delayed event (candidate α-decay of ^{212}Po, black histogram) of TCE from the first source. Vertical dashed lines delimit the energy cuts used in the analysis for the β candidate; no cuts were used for the second event.

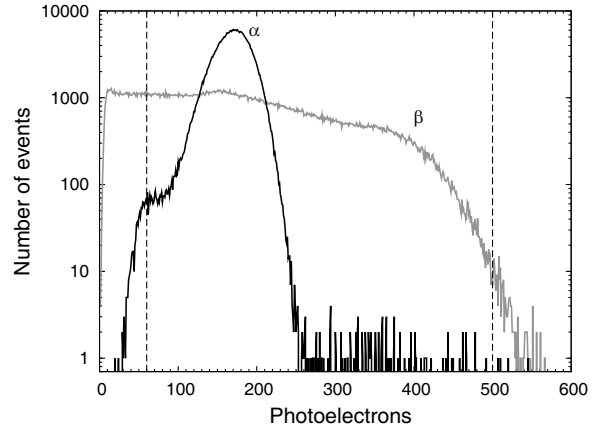

Fig. 3. Energy spectrum for the prompt (candidate β-decay of ^{212}Bi, gray histogram) and delayed event (candidate α-decay of ^{212}Po, black histogram) of TCE from the second ^{212}Po source. Vertical dashed lines delimit the energy cuts used in the analysis for the β candidate; no cuts were used for the second event.

Table 3. Summary of mean-life results. Final results come from the mean value approach with energy cuts and also report systematic errors; the ^{212}Po results include a -0.4 ns correction for systematics as discussed in the text.

Method	^{214}Po [μs]	^{212}Po [ns]	
		Source 1	Source 2
Analytical fit	236.26 ± 0.47		
χ^2 with penalty		426.8 ± 1.3	424.2 ± 1.1
χ^2 with penalty and energy cuts	236.00 ± 0.43	426.5 ± 1.4	424.1 ± 1.2
Mean value	236.85 ± 0.42	426.8 ± 1.5	424.2 ± 1.1
Mean value with energy cuts	236.00 ± 0.42	426.5 ± 1.4	424.2 ± 1.1
Final result	$236.00 \pm 0.42 \pm 0.15$	$426.5 \pm 1.4 \pm 1.2$	$424.2 \pm 1.1 \pm 1.2$
		$425.1 \pm 0.9 \pm 1.2$	

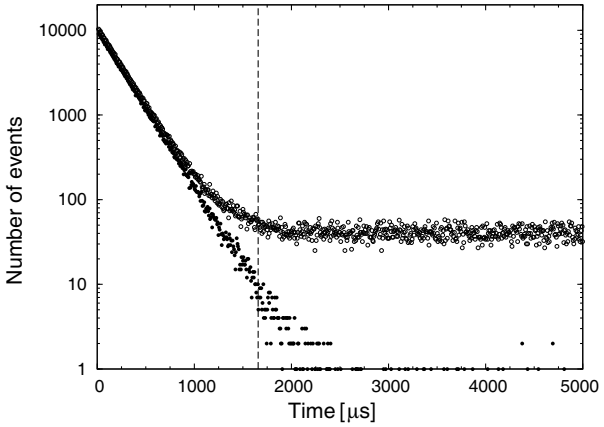

Fig. 4. Data from the ^{214}Po source with 1000 bins between 5 and 7605 μs are shown up to 5000 μs. Number of TCE's as a function of the time difference t between the first and the second decay. Filled (open) dots show data with (without) the energy cuts reported in the text. Vertical lines delimit a seven-lifetime window.

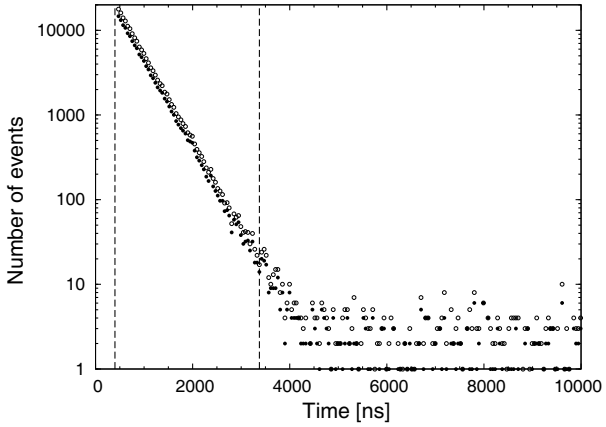

Fig. 5. Data from the first ^{212}Po source with 1000 bins between 400 and 48000 ns are shown up to 10000 ns.Number of TCE's as a function of the time difference t between the first and the second decay. Filled (open) dots show data with (without) the energy cuts reported in the text. Vertical lines delimit a seven-lifetime window.

3.1 χ^2 with penalty factor

In order to suppress the background contamination, polonium candidates are selected by looking for pairs of time correlated events (TCE), in time windows of 1.7 ms for the ^{214}Po and 3 μs for the ^{212}Po analysis. Potential contaminations due to random coincidences are further reduced by applying energy cuts: [250–850] and [150–280] p.e. for the ^{214}Bi and ^{214}Po (fig. 1), and [60–500] p.e. for the ^{212}Bi and no cut for ^{212}Po (figs. 2 and 3). These energy cuts reduce the background by about two orders of magnitude in the ^{214}Po analysis, and by a factor ≈ 2 for ^{212}Po. The distributions of the measured time differences between the two events, with and without the energy cuts, are shown in figs. 4 and 5, respectively.

The mean lifetime is then evaluated by minimizing

$$\chi^2(n_0, \lambda, b_0) = \chi^2_0(n_0, \lambda, b_0) + \left(\frac{b_0 - \bar{b}}{\Delta\bar{b}}\right)^2, \qquad (1)$$

where n_0 is the number of polonium decays, λ the decay constant, and b_0 the background due to accidental coincidences. The $\chi^2_0(n_0, \lambda, b_0)$ is estimated by using the exponential model

$$b_0 + n_0 \exp(-\lambda t). \qquad (2)$$

The expected value of the background $\bar{b}$ with error $\Delta\bar{b}$ is estimated by measuring it independently in the off-time windows ([3.0–7.6] ms for the ^{214}Po case, and [8.0–48.0] μs for the ^{212}Po one, scaled to the length of the time windows used for the measurements ([0.005–1.705] ms and [0.4–3.4] μs, respectively). Since the electronics acquire only the first event following the bismuth candidate, the background related component is Poissonian and has an exponential behavior,

$$b_0 e^{-b_1 t}, \qquad (3)$$

where b_1 is the background rate. However, all our background data samples do not show deviations from the constant accidental background ($b_1 = 0$ within the errors in the selected time windows), as expected given the low background rate.

Total-number-of-events/estimated-background-events in the selected time windows are about $3.1 \times 10^5/17$ with energy cuts for ^{214}Po; $9.4 \times 10^4/43$ ($1.1 \times 10^5/86$) with (without) energy cuts for the first ^{212}Po source; $1.4 \times 10^5/43$ ($1.7 \times 10^5/173$) with (without) energy cuts for the second ^{212}Po source.

The s^{214}Po mean-life obtained this way is $(236.00 \pm 0.43)\,\mu$s with energy cuts, while the measured mean-lives for the two samples of ^{212}Po are (426.9 ± 1.4) ns and (424.5 ± 1.2) ns with energy cuts, and (427.2 ± 1.3) ns and (424.6 ± 1.1) ns without energy cuts.

3.2 Analytical fit

In this approach, no energy cuts have been applied to the data, which are fit with an analytical model, including an exponential decaying background,

$$n_0 e^{-\lambda t} + b_0 e^{-b_1 t}. \tag{4}$$

The method was applied only to the ^{214}Po data in the energy window [0.005–7.605] ms, since in this case there are both signal dominated and background dominated bins (see fig. 4).

Total-number-of-events/estimated-background-events in the selected time window are about $3.9 \times 10^5/4.4 \times 10^4$. No deviation from constant background is detected.

The so-obtained ^{214}Po mean-life is $(236.26 \pm 0.47)\,\mu$s.

This fit and the ones in the previous subsect. 3.1 are performed minimizing the χ^2 using the binned likelihood method. Results are stable when changing the number of bins, and the χ^2's are compatible with statistical fluctuation around the value expected for the appropriate number of degrees of freedom.

3.3 Unbinned mean value

For the ideal case of exponentially distributed data with no background and an infinite time window, the average time $\sum_{i=1}^{n} t_i/n$, where t_i is the time of the i-th event and n the number of events, is the best estimate of the lifetime τ with the smallest variance $\sigma^2 = \tau^2/n$ [23–25].

Since our data are close to this ideal case, thanks to the favorable signal-to-background ratio, as shown in figs. 4 and 5, we can apply the *unbinned mean value* approach with two small corrections: one for the finite width of the time window and the other for a constant background contribution.

The correction for the finite time window can be calculated analytically: defining s the average decay time in the data window of length T, the relation between the infinite window lifetime τ and s is

$$s = \frac{1}{n}\sum_{i=1}^{n} t_i = \tau - \frac{T}{e^{T/\tau} - 1}. \tag{5}$$

A $T \approx 7\tau$ window, used for both polonium measurements, requires a correction of about +0.6%.

In order to check the stability of this approach, we split the data in 5 independent equal-size subsets and apply eq. (5) to each of them. The estimated variance of the mean is $\sigma^2 = \sum_{i=1}^{5}(\tau_i - \overline{\tau})^2/(5(5-1))$, where τ_i ($i = 1, \ldots, 5$) are the 5 results and $\overline{\tau}$ is their average.

This approach has been implement first without energy cuts, and then applying the same energy cuts already reported in subsect. 3.1 for the χ^2 with penalty approach. The largest correction for the background is found for the ^{214}Po source without energy cuts, where the signal-to-background ratio (S/B) is ≈ 36. The subtraction of a constant background with a number of events about 2.7% of the signal implies a correction to the lifetime of about −7%, which is then equal to $(236.85 \pm 0.42)\,\mu$s. This correction is reduced to about 10^{-4} with the energy cuts (S/B $\approx 1.82 \times 10^4$), resulting in a ^{214}Po mean-life equal to $(236.00 \pm 0.42)\,\mu$s.

Background corrections for the ^{212}Po sources are of the order of 10^{-4} even without energy cuts. The results for the first sample, with (S/B $\approx 2.2 \times 10^3$) and without (S/B $\approx 1.3 \times 10^3$) the energy cuts, are (426.9 ± 1.4) ns and (427.2 ± 1.5) ns, respectively. The same analysis on the second ^{212}Po sample leads to a slightly lower values: (424.6 ± 1.1) ns and (424.6 ± 1.1) ns. In this case, the S/B ratios are $\approx 3.3 \times 10^3$ with and $\approx 1.0 \times 10^3$ without the energy cuts.

Time windows for signal and background and corresponding numbers of events are the same reported in subsect. 3.1 where the χ^2 with penalty approach is discussed.

4 Systematic errors

The models, described in the previous section, do not include several detector effects. In particular, the PMT jitter ($\lessapprox 1.5$ ns, which is the quality threshold for selecting PMT's in CTF [26]), photon scattering, absorption and remission, and time binning on samples. Further, the maximum difference (≈ 40 cm) in the photon paths to reach the PMTs induces a spread in the time distribution of about 0.8 ns. Another smearing is due to the TDC (LeCroy CAMAC 4208, 8 Channel Wide Range Real-Time), with a time resolution of 1 ns, which implies a further $\sigma = 0.29$ ns. A detailed Monte Carlo package has been developed in order to estimate the translation of these smearing effects into an overall systematic error.

In order to calibrate the Master Clock oscillator of the TDC and to check its stability we performed a set of measurements using the same "GPS disciplined high precision counter system" utilized for high precision measurements of the neutrino speed [27]. We have found that the actual, measured frequency of the Master Clock Oscillator deviates by −47.5 ppm from its nominal value at ambient temperature of 23 °C. The short-term oscillator stability during a two-hour run after stabilization was better than ±0.08 ppm. The long term drift of the central value of the oscillator frequency was less than ±1.5 ppm during a 24 hour run. We have found that the temperature dependency of the oscillator frequency was 0.05 ppm per

degree. Furthermore, we have observed a 1σ RMS short-term jitter in the master oscillator of 15 picoseconds. Taking into account the observed good stability in these measurements, the standard factory values, usually declared for precision AT cut non-oven-stabilized oscillators, crystal aging and temperature changes, our sistematic error due to the TDC is within ± 20 ppm. This "worst case" scenario implies absolute errors of $\pm 0.005\,\mu$s for ^{214}Po and ± 0.009 ns for ^{212}Po measurement.

Another subtle effect is due to the difference in the scintillation-photon time distributions after a β- or α-decay.

The simulation takes into account all the mentioned effects and yields an overall systematic shift of about $(+0.4 \pm 0.1)$ ns for the unbinned mean value approach. Therefore, 0.4 ns are subtracted from our final results for ^{212}Po (see table 3).

We further studied the result stability by varying the lower threshold of the time acquisition window, from 0.2 to 80 μs and from 0.35 to 0.65 μs for the ^{214}Po and ^{212}Po cases, respectively; in addition, we varied also the upper limit for the ^{212}Po time window from 3 to 3.5 μs. We also varied the energy cuts: the lower (higher) charge threshold of the first event in the range 200–300 p.e. (750–850 pe.e.) for ^{214}Po, and with and without energy cuts on the first event for ^{212}Po; the lower (higher) charge threshold of the second event in the range 130–150 p.e. (180–280 pe.e.) for ^{214}Po, while we did not apply any cut for ^{212}Po. We adopted a conservative definition of the systematic error as half of the spread of the measured lifetimes obtained by applying such different data selection criteria. The overall estimated systematic errors are 0.15 μs and 1.2 ns for ^{214}Po and ^{212}Po, respectively.

5 Results and comparison with previous measurements

The different approaches, used in this analysis, provide compatible results within 1.5σ, as shown in table 3. The best results are obtained by means of the *unbinned mean value* method with energy cuts, which provides the smallest statistical uncertainties; 0.4 ns systematic has been subtracted from the the ^{212}Po values. Since the measurements with the two ^{212}Po sources are statistically independent, we combined the results with the weighted average. The final ^{214}Po and ^{212}Po mean-life results are

$$\tau(^{214}\mathrm{Po}) = 236.00 \pm 0.42(\mathrm{stat}) \pm 0.15(\mathrm{syst})\,\mu\mathrm{s},$$
$$\tau(^{212}\mathrm{Po}) = 425.1 \pm 0.9(\mathrm{stat}) \pm 1.2(\mathrm{syst})\,\mathrm{ns}.$$

We report the comparisons of our results with the best measurements found in literature in tables 1 and 2, where statistical and systematic errors are combined.

The ^{214}Po lifetime measured by von Dardel [2] is as accurate as our measurement, although based on larger statistics, corresponding to $\approx 3 \times 10^6$ events, and with the same acquisition window time length (7 lifetimes). The net advantage of the CTF measurement is the favorable signal-to-background ratio, higher by more than 3 order of magnitude.

All available experimental data on ^{214}Po are reviewed and combined in the Christe *et al.* [10], and Wu *et al.* [9] compilations. The first one combines all the existing measurements, finding $\tau = 234.1 \pm 1.7\,\mu$s. The second takes into account only the three most precise measurements [2, 5,6], obtaining $\tau = 237.0 \pm 2.9\,\mu$s. Note that both compilations rely on techniques for evaluation of data that include some form of Limitation of Relative Statistical Weight preventing a single measurement to dominate the result: if necessary, the smallest error is increased so that the corresponding weight is at most 0.5. This is the reason the resulting average and error are not dominated by the one of von Dardel [28], which would have by far the smallest error. After including the present measurement in these compilations, the average and the error should be determined almost only by the two measurements with smallest errors, ours and von Dardel's, with comparable weights, reducing the final uncertainty on ^{214}Po lifetime by a factor ≈ 6 (the adopted number and error depending on the evaluation technique). A recent experimental test of the time stability of ^{214}Po half-life [8] has not yet studied the systematic error of the absolute value. If one uses the discrepancy of their results from two difference sets of data as an estimate of the error, the resulting mean life, $\tau = 235.9 \pm 1.1\,\mu$s, is compatible with ours.

Similarly, in the case of the ^{212}Po, seven measurements have be found in the literature [11–16], as shown in table 2. Our result agrees with the most accurate measurement by Sanyal [15], where the statistical sample is comparable ($\approx 2 \times 10^5$ events), but the acquisition time window is limited to about 4 lifetimes and the signal-to-noise ratio is poorer. All the other measurements show slightly higher central values, with larger uncertainties, and compatible with the present work at 2σ level.

In the work by Browne *et al.* [17] the average of five measurements [11,13–16] is quoted and it is equal to $\tau = 431 \pm 3$ ns. Another work by Nichols *et al.* [18] takes into account six measurements [11–15], finding $\tau = 433 \pm 32$ ns.

As in the ^{214}Po case, evaluation techniques avoid that a single measurement has a weight larger than 0.5. The present result, when included in these compilations, should give the more important contribution together with the measurement of Sanyal [15] to the adopted lifetime, which will become lower, and to the uncertainty, which will be reduced.

In conclusion, thanks to extreme radio-purity of the CTF detector and to a long expertise in source preparation and insertion systems, new accurate measurements of the ^{214}Po and ^{212}Po lifetimes have been provided.

We acknowledge the generous support of the Laboratori Nazionali del Gran Sasso and we thank the funding agencies: INFN (Italy), NSF (USA), BMBF, DFG and MPG (Germany), Rosnauka (Russia), the Ministry of Education and Science (Russia), and MNiSW (Poland). We are grateful for enlightening discussions with and the valuable comments of E. Bellotti and B. Ricci.

References

1. G. Alimonti *et al.*, Nucl. Instrum. Methods A **406**, 411 (1998).
2. Guy von Dardel, Phys. Rev. **79**, 734 (1950).
3. René Ballini, Ann. Phys. **8**, 441 (1953).
4. K.W. Ovilvie, Proc. Phys. Soc. (London) **76**, 299 (1960).
5. T. Dobrowolski, J. Young, Proc. Phys. Soc. (London) **77**, 1219 (1961).
6. A. Erlik, J. Felsteiner, H. Lindenman, M. Tatcher, Nucl. Instrum. Methods **92**, 45 (1971).
7. J.W. Zhou *et al.*, Nucl. Instrum. Methods Phys. Res. A **335**, 443 (1993).
8. E.N. Alexeyev, J.M. Gavriljuk, A.M. Gangapshev, A.M. Gezhaev, V.V. Kazalov, V. Kuzminov, S.P. Yakimenko, S.I. Panasenko *et al.*, Astropart. Phys. **46**, 23 (2013).
9. S.-C. Wu, Nucl. Data Sheets **110**, 681 (2009).
10. V. Christé, M.M. Bé, ^{214}*Po - Comments on evaluation of decay data*, Table de Radionucléides, LNE - LNHB/CEA (2007).
11. D.E. Bunyan, A. Lundby, D. Walker, Proc. Phys. Soc. (London) A **62**, 253 (1949).
12. F.C. Flack, J.E. Johnson, Proc. Phys. Soc. (London) **79**, 10 (1962).
13. G. Astner, I. Bergstrom, L. Eriksson, U. Fagerquist, G. Holm, A. Persson, Nucl. Phys. **45**, 49 (1963).
14. G.W. McBeth, R.A. Winyard, Int. J. Appl. Radiat. Isot. **23**, 527 (1972).
15. S. Sanyal, R.K. Garg, S.D. Chauhan, S.L. Gupta, S. Pancholi, Phys. Rev. C **12**, 318 (1975).
16. H. Bohn, E. Endres, T. Faestermann, P. Kienle, Z. Phys. A **302**, 51 (1981).
17. E. Browne, Nucl. Data Sheets **104**, 427 (2005).
18. A.L. Nichols, ^{212}*Po - Comments on evaluation of decay data*, Table de Radionuclé ides, LNE - LNHB/CEA (2010).
19. Borexino Collaboration (G. Alimonti *et al.*), Astropart. Phys. **8**, 141 (1998).
20. G. Zuzel, H. Simgen, G. Heusser, Appl. Radiat. Isot. **61**, 197 (2004).
21. G. Fiorentini *et al.*, Phys. Rev. C **81**, 034602 (2010).
22. Borexino Collaboration (G. Bellini *et al.*), Eur. Phys. J. C **54**, 61 (2008).
23. R. Peierls, Proc. R. Soc. A **149**, 467 (1935).
24. A.H. Jeffrey, Nucl. Instrum. Methods **81**, 155 (1970).
25. A.H. Jeffrey, Nucl. Instrum. Methods **81**, 253 (1970).
26. A. Ianni, P. Lombardi, G. Ranucci, O.Ju. Smirnov, Nucl. Instrum. Methods A **537**, 683 (2005).
27. Borexino Collaboration (P. Alvarez Sanchez *et al.*), Phys. Lett. B **716**, 401 (2012).
28. Guy von Dardel, Ark. Fys. **2**, 337 (1951).